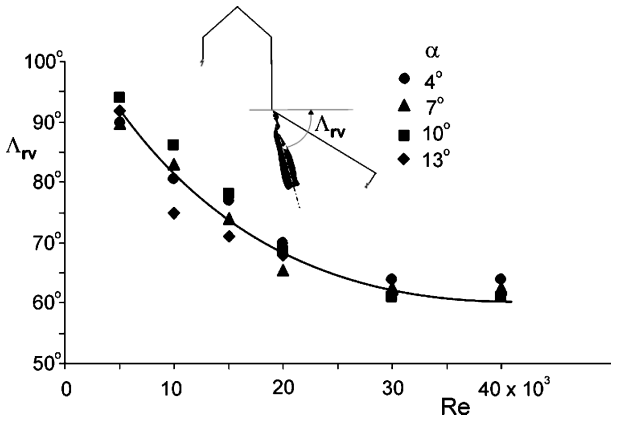


**Fig. 5 Effective sweep angle $\Lambda_{rv}$ of vortex formed from wing root as a function of Reynolds number *Re* based on chord *C* of planform.**

further increases in Reynolds number are likely to yield only small decreases in $x_b/C$.

In the foregoing, emphasis has been on the onset of pronounced undulations/breakdown for the vortices emanating from the apex of the planform. It is, however, possible to discern the onset of vortex breakdown of the wing root vortex at higher values of Reynolds number. For example, see $\alpha = 7$ deg, $Re = 3 \times 10^4$. This onset of breakdown at $\alpha = 7$ deg appears to move closer to the wing root for an increase of Reynolds number *Re* to $4 \times 10^4$.

## VI. Angles of Inclination of Wing Root and Apex Vortices

Another indicator of the effect of Reynolds number is the angle of inclination of the vortex emanating from the wing root. It is possible to determine an effective sweep angle $\Lambda_{rv}$ of this vortex core, as defined in the schematic of Fig. 5. As indicated, it is the angle between a line drawn through the center of the vortex core (or, in cases where the core exhibits a spiral, through the center of the spiral) and a line that is perpendicular to the plane of symmetry of the wing. In other words, this effective sweep angle is equivalent to the definition of sweep angle of the leading edge of a delta wing. The dye images of Figs. 2a and 2b indicate that, at lower values of Reynolds number extending up to $Re = 2 \times 10^4$, the value of the effective sweep angle $\Lambda_{rv}$ varies substantially, whereas at $Re = 3 \times 10^4$ and $4 \times 10^4$ little change is evident, indicating that an asymptotic value has been attained. The plot of Fig. 5 clarifies this trend, and emphasizes that the angle $\Lambda_{rv}$ is a mild function of angle of attack $\alpha$. This observation contrasts with the strong effect of $\alpha$ on the onset of pronounced undulations/breakdown $x_b/C$ indicated in Fig. 4. Regarding the values of sweep angle of the vortices from the apex of the wing, it is predominantly a function of Reynolds number. At a given Reynolds number, over the values of $\alpha = 4$–13 deg, the range of values of sweep angle $\Lambda_{av}$ of the apex vortex are as follows. For $Re = 10{,}000$, $14^\circ \le \Lambda_{av} \le 17^\circ$; for $Re = 15{,}000$, $15^\circ \le \Lambda_{av} \le 20^\circ$; for $Re = 20{,}000$, $17.5^\circ \le \Lambda_{av} \le 20^\circ$; for $Re = 30{,}000$, $21^\circ \le \Lambda_{av} \le 23^\circ$; and for $Re = 40{,}000$, $27.5^\circ \le \Lambda_{av} \le 32^\circ$.

## VII. Conclusions

This Reynolds number dependence of the vortex patterns on a representative UCAV planform, which is distinguished by small sweep angles, can be defined in terms of the onset of pronounced instability/abrupt breakdown of the vortices from the apex of the main body, the effective sweep angle of the vortices from the wing root, and the degree of interaction of the vortices from the apex and the wing root. At relatively low angle of attack, the onset of pronounced instability/breakdown is highly sensitive to Reynolds number, whereas at relatively high angle of attack, it is much less sensitive. The effective sweep angle of the wing root vortex is only a mild function of angle of attack; it is predominantly a function of Reynolds number and tends toward an asymptotic value at high Reynolds number. The Reynolds number at which the vortices from the apex and the wing root cease to interact decreases substantially with a decrease in angle of attack.

## Acknowledgments

The authors gratefully acknowledge the support of the U.S. Air Force Office of Scientific Research, under Grant F49620-02-1-0061, monitored by John Schmisseur.

## References

[1]Hebbar, S. K., Platzer, M. F., and Fritzelas, A. E., "Reynolds Number Effects on the Vortical-Flow Structure Generated by a Double-Delta Wing," *Experiments in Fluids*, Vol. 28, 2000, pp. 206–216.

[2]Verhaagen, N. G., "Effects of Reynolds Number on Flow over 76/40-Degree Double-Delta Wings," *Journal of Aircraft*, Vol. 39, No. 6, 2002, pp. 1045–1052.

[3]Visser, K. D., and Washburn, A. E., "Transition Behavior on Flat Plate Delta Wings," AIAA Paper 94-1850, June 1994.

[4]Verhaagen, N. G., Jenkins, L. N., Kern, S. B., and Washburn, A. E., "A Study of the Vortex Flow over a 76/40-deg Double-Delta Wing," AIAA Paper 95-0650, Jan. 1995.

[5]Gordnier, R. E., and Visbal, M. R., "Higher-Order Compact Difference Scheme Applied to the Simulation of a Low Sweep Delta Wing Flow," AIAA Paper 2003–0620, Jan. 2003.

[6]Yaniktepe, B., and Rockwell, D., "Flow Structure in Regions of Vortex Breakdown and Stall on a Delta Wing of Low Sweep Angle," *AIAA Journal*, Vol. 42, No. 3, 2004, pp. 513–523.

# Suppression of Wing Rock Using Artificial Neural Networks and Fuzzy Logic Controller

A. G. Sreenatha* and P. P. Wong†
*University of New South Wales,*
*Canberra, Australian Capital Territory 2600, Australia*
and
J. Y. Choi‡
*Seoul National University,*
*Seoul 151-600, Republic of Korea*

## Introduction

THE dynamics of single delta free to roll model at high angles of attack show a nonlinear phenomenon known as wing rock. Wing rock is a complicated aerodynamic phenomenon, characterized by self-induced limit-cycle roll oscillations. Aerodynamic suppression, the suppression of wing rock by the direct control and manipulation of leading-edge vortices, has demonstrated to be effective in controlling wing rock in slender delta wings.[1–5] A particular type of aerodynamic suppression known as recessed angle spanwise blowing (RASB), has been implemented by Sreenatha and Ong[5] via a simple rule-base controller. Experimental results in the wind tunnel revealed the effectiveness of RASB at one angle of attack and freestream velocity. Currently, the mathematical

Received 4 December 2003; revision received 24 February 2004; accepted for publication 24 February 2004. Copyright © 2004 by the authors. Published by the American Institute of Aeronautics and Astronautics, Inc., with permission. Copies of this paper may be made for personal or internal use, on condition that the copier pay the $10.00 per-copy fee to the Copyright Clearance Center, Inc., 222 Rosewood Drive, Danvers, MA 01923; include the code 0021-8669/04 $10.00 in correspondence with the CCC.

*Senior Lecturer, School of Aerospace, Civil and Mechanical Engineering, University College, Northcott Drive.

†Student, School of Aerospace, Civil and Mechanical Engineering, University College, Northcott Drive.

‡Associate Professor, School of Electrical and Computer Engineering, Kwanak P.O.Box 34.

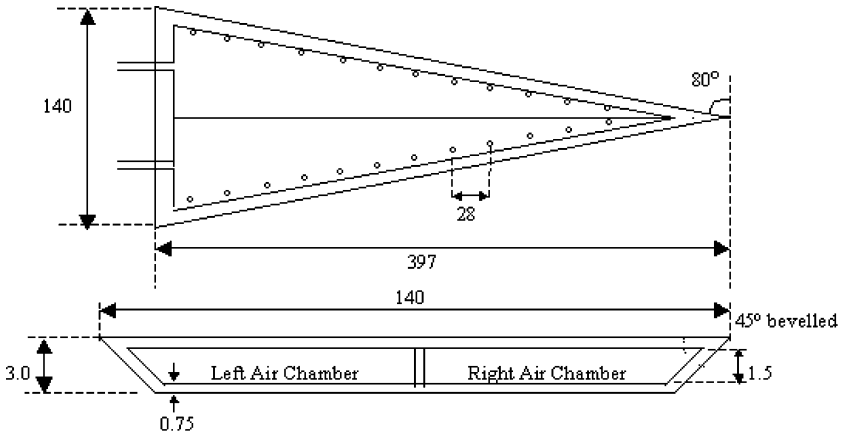


**Fig. 1 Schematic plan and back view of the slender delta wing model; all dimensions in millimeters, not to scale.**

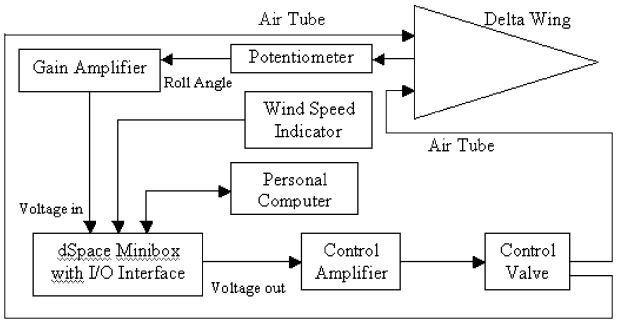


**Fig. 2 Block diagram of experimental setup.**

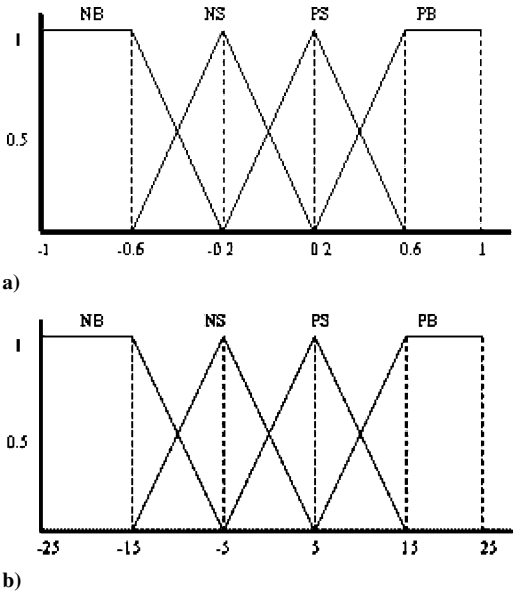


**Fig. 3 Membership function of a) roll angle and b) roll rate.**

model for wing rock is only approximate.[6,7] Intelligent controllers promise better performance and robustness, in the absence of an accurate model. As such, intelligent systems such as artificial neural networks (ANN) and fuzzy controllers have become popular design paradigms for wing rock control. Sreenatha and Lim[8] have presented a fuzzy logic controller (FLC) for wing rock. Numerical results have been presented to demonstrate its robustness. Joshi et al.[9] presented a single-neuron controller for wing rock. Numerical and experimental results demonstrated the robustness of the controller at a few angles of attack and initial conditions. However, the controller was non-aerodynamic in nature.

This Note presents the experimental implementation of RASB, using FLC and ANN controllers on a slender delta wing in a low-turbulence wind tunnel. Effectiveness of the controllers is demonstrated by the suppression of wing rock in experimental simulations. Assessment of the controller's performance over a range of flight conditions with different angles of attack and freestream velocities highlight the robust nature of the intelligent controllers and the suitability of such techniques to be implemented in aircrafts.

## Experimental Setup

An 80-deg swept angle delta wing with an aspect ratio of 0.705 constructed out of aluminium is employed for the present study. The wing's internal structure includes two symmetrical longitudinally separated chambers providing two cavities for air passage through the left and right portion of the wing. There are drilled, in each side of the wing at the same bevelled angle of 45 deg to the wing surface, 12 blowing ports 1.0 mm in diameter, as shown in Fig. 1. This slender delta wing is mounted on low-friction bearings to allow it to rotate freely about its longitudinal axis. A dSpace Minibox™ provides the I/O interface, which is used for data acquisition and processing. Online tuning and manipulation of design parameters are carried out on the personal computer linked to the dSpace Minibox, which also stores and displays the data. The block diagram of the experimental setup is shown in Fig. 2. The electronic proportional directional control valve has two output channels that are connected to each side of the wing via rubber tubes. The valve-slide stroke of this control valve can be controlled to a specified setpoint by an analog electrical input signal. An electrical input signal generated from the controller in the personal computer via dSpace commands the switching of the valve-slide stroke between its two output channels to supply the air into either side of the wing at the required pressure. The critical angle at 18 m/s, where wing rock is experienced by the model, is 19 deg. For analysis of the controllers, an operating envelope of 21–23 deg between freestream velocities of 18–33 m/s is selected.

## FLC Design

The Takagi–Sugeno implication system is used because it provides a more efficient defuzzification process where the required output is constant or linear (see Ref. 10), which is the case for the proportional directional valve. The membership functions of the FLC are shown in Fig. 3. The domains used in the membership function for $\phi$ and $\dot{\phi}$ (roll angle and roll rate) are representative of the maximum values of roll and roll rate characteristics of wing rock experienced on the experimental model within the operating envelop. The convention is such that roll angle is positive when the wing is rolling to the right and vice versa. The domain of the control input $u$ relates to the proportional and directional properties of the control valve. The magnitude of $u$ determines the amount of valve opening, where value of 5 indicates that the valve is fully opened. The sign of $u$ determines the direction, where negative indicates the valve is opened on the left, effecting blowing on the left portion of the wing. The output membership function consists of three constants: blow left (BL), blow right (BR), and no blowing (ZO),

with corresponding values of −5, 5, and 0. This is reflective of the proportional and directional characteristics of the control valve described earlier. The output is determined from the set of fuzzy rules summarized in Fig. 4. For example, if $\phi$ is negative big (NB) and $\dot{\phi}$ is NB then $u$ is BL. Previous pressure transducer studies involving the control system highlighted the significance of electromechanical lag present in the servocontrol valve.[5] These rules are modified from the simple rule base used in Ref. 5 to incorporate advance blowing to account for the electromechanical lag present in the system. The control logic is shown in Fig. 5. The FLC was initially unable to achieve suppression of wing rock experienced by the experimental model. There was no significant reduction of wing rock amplitude with the application of the designed FLC under all conditions within the operating envelope. Further investigations revealed that the advance blowing is insufficient to overcome the electromechanical lag in the system. A delay function is added to the control system, which allows real-time alteration of the delay time imposed on the control input. When the correct delay time is chosen, the onset of physical blowing at the wing can be altered accordingly, to ensure that blowing occurs at the specific points within the wing rock cycle. Subsequent wind-tunnel experiments with varying values of delay time revealed significant improvement in controller performance. The effect of delay times on wing rock suppression is clearly shown in Fig. 6. Further experimentations with the FLC design revealed that the required delay time is a function of freestream velocity. Furthermore, the delay time required remains unchanged at different angles of attack (AOA). The variation of delay times with freestream velocity is entered into a time-lag database in the form of a lookup table. The database outputs a delay time based on the input, which in this case is the freestream velocity. The addition of this time-lag database imparts automation to the FLC. This automated FLC is subjected to real-time experimental simulations at all flight conditions of the operating envelop specified in the design criteria. The experimental results revealed suppression of wing rock throughout the operating envelop. Examples of successful suppression are included in Fig. 7.

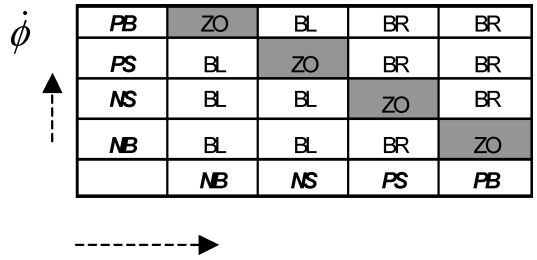


**Fig. 4 Fuzzy control table.**

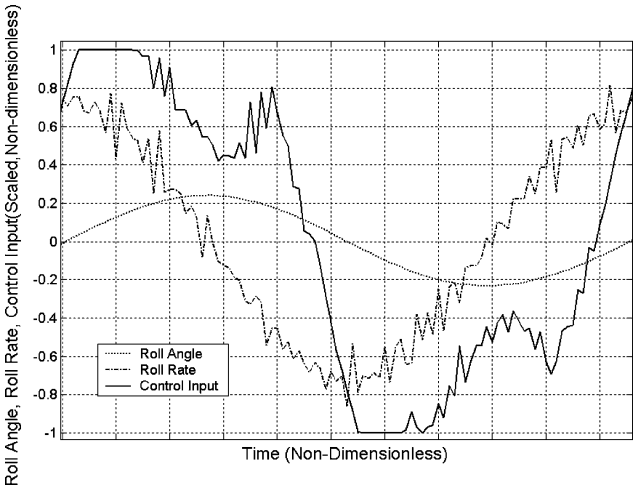


**Fig. 5 Control logic of FLC.**

## ANN Design

A feedforward ANN architecture is featured here, with different processing neurons organized in layers. Increasing the number of layers and neurons can enhance the capability of feedforward-type ANN to learn and represent machine intelligence.[11] The inputs to the ANN in the present work are $\phi$ and $\dot{\phi}$ and the output is $u$, the control input. Initially, the knowledge-base used to provide the training information is the rule-base used in Ref. 5, a specification of the required control input at a particular instance, based on the inputs to the system. A backpropagation training algorithm is used to find the weights associated with the inputs of the controller with the training samples derived from the rule base. This training process allowed the ANN to learn the examples taught by the rule base and build its own continuous model of the control strategy. However, this trained ANN was unable to achieve wing rock suppression on the experimental model over the desired operating envelope because the electromechanical lag was not accounted for by the rule base. Attempts to incorporate phase shift into the training rule base proved unfruitful and time consuming. The implementation of lag times into the training algorithm requires extensive online fine tuning of the ANN controller and retraining with phase-shifted rule bases. This approach was deemed too time consuming. Training was then

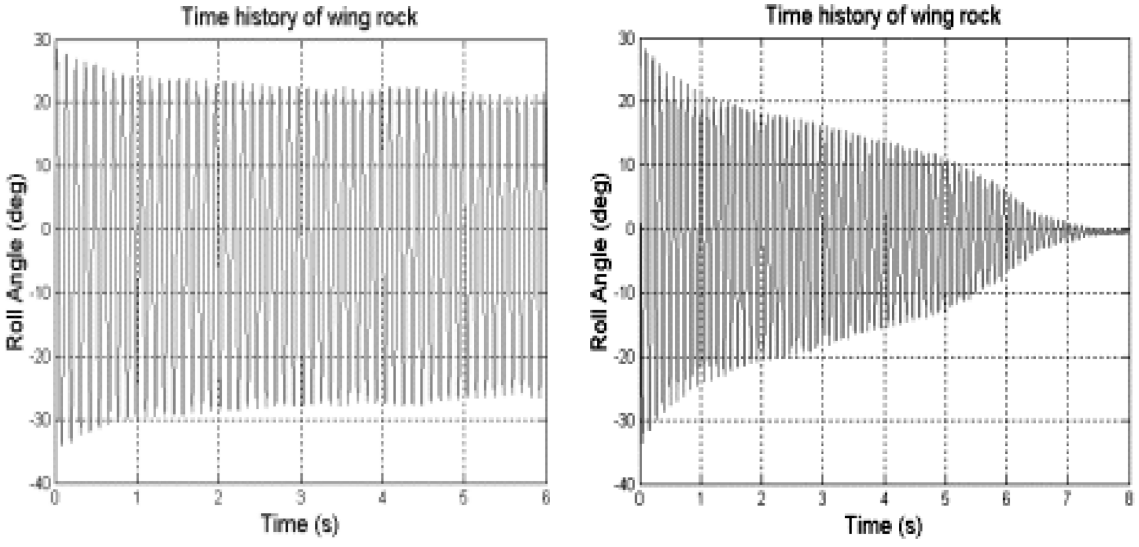


a) b)

**Fig. 6 Wing rock motion at 22-deg AOA, 28 m/s with FLC applied: a) with no delay time and b) with 15-ms delay time.**

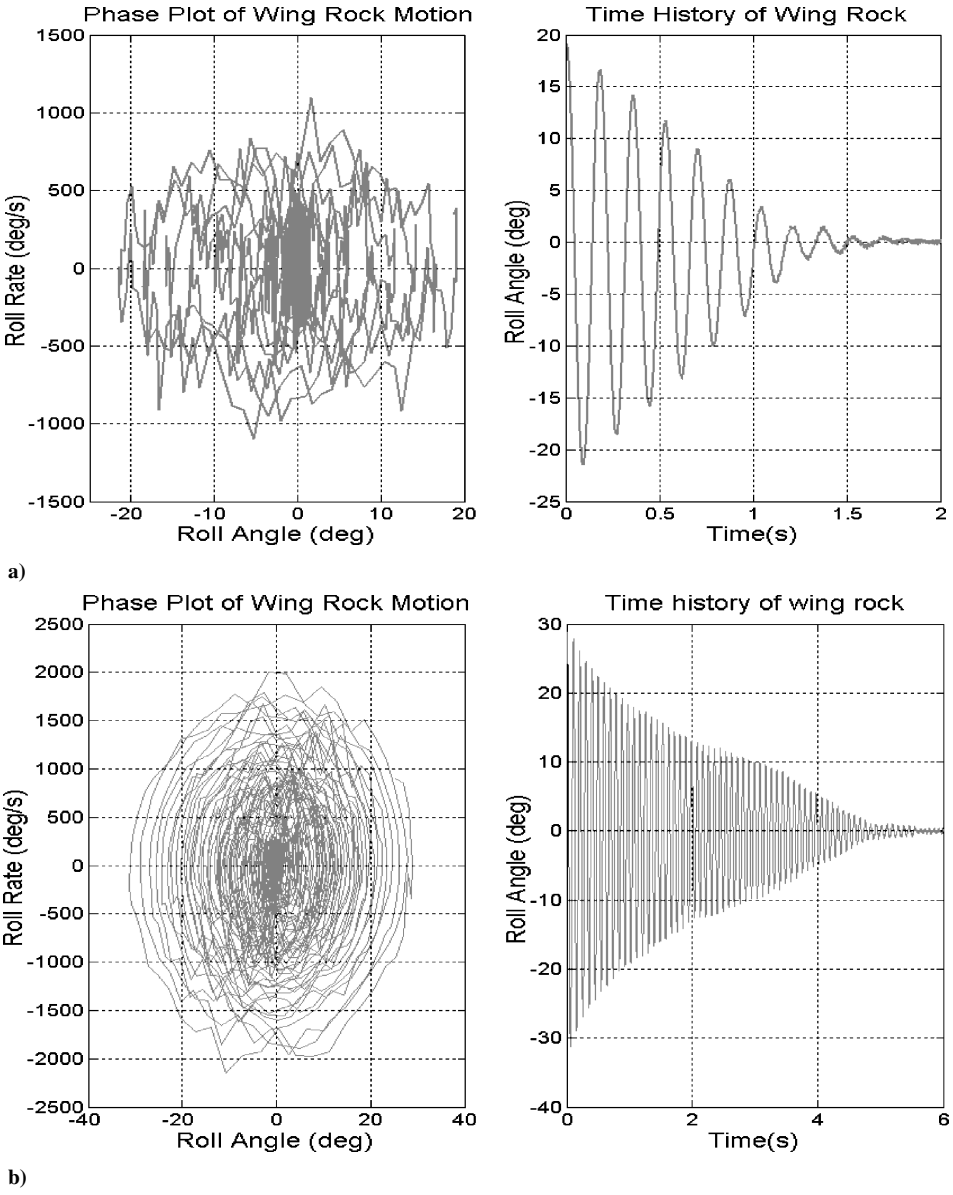


**Fig. 7 Wing rock suppressed at a) 21 deg AOA, 18 m/s, and b) 23 deg AOA, 33 m/s.**

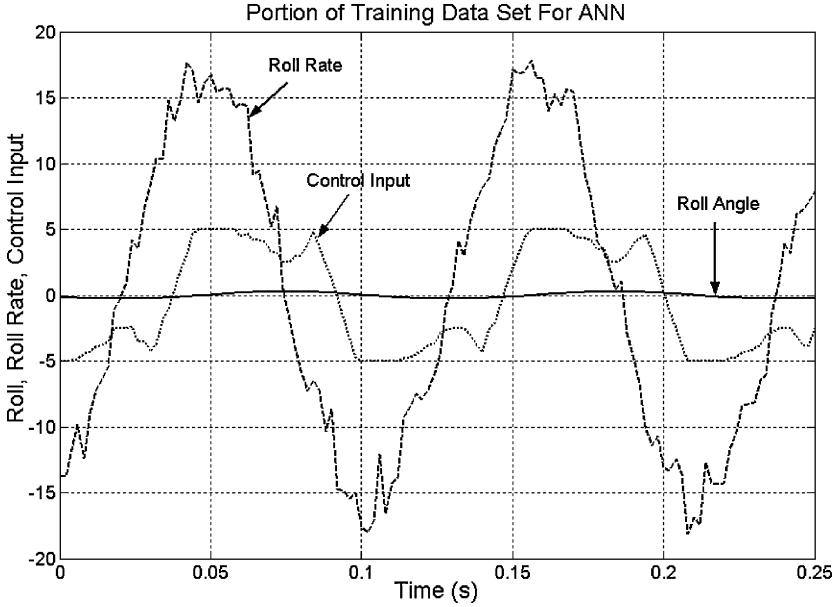


**Fig. 8 Part of a training data set for ANN.**

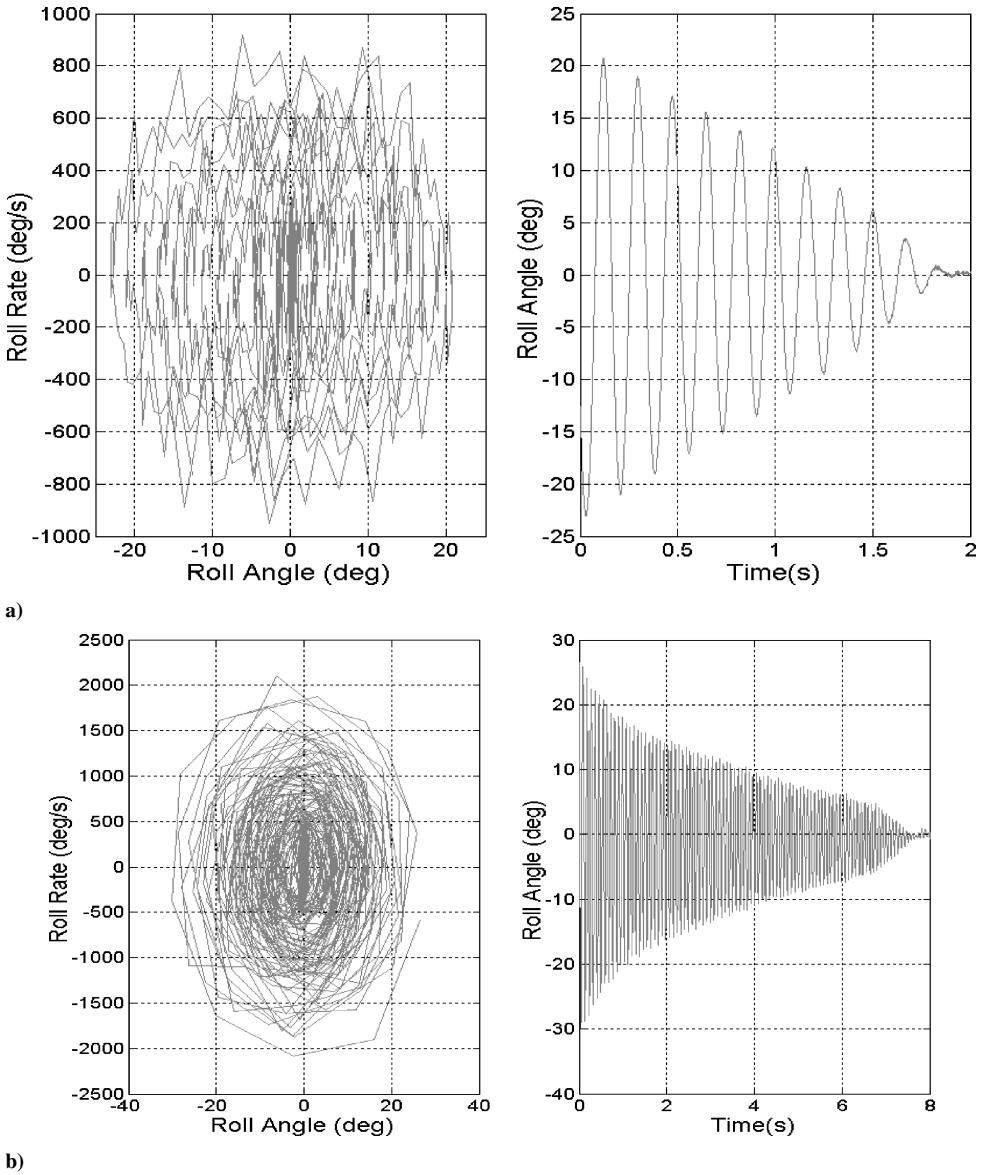


**Fig. 9 Suppression of wing rock at a) 21-deg AOA, 18 m/s and b) 22.5-deg AOA, 32 m/s.**

carried out with the I/O data from the FLC experiments, whereby electromechanical lag is automatically accounted for. However, each fine-tuned fuzzy controller is only able to suppress wing rock at the condition it is tuned at. Figure 8 shows part of a training data set for the ANN. Because of the nonlinearity of the I/O relationship, additional neurons and layers have to be used in the architecture to improve the learning ability of the ANN. Experimental data from different flight conditions were used for training the ANN and testing. ANN trained at different flight conditions has different ability to suppress wing rock over a different range of freestream velocity. Extensive trials were conducted to investigate the performance of the ANN trained. Table 1 shows the most significant results obtained. The results suggest that it might be possible to produce an ANN that is capable of effecting desired wing rock control over the entire range of operating conditions by combining the training data from the two flight conditions identified. To ensure a better learning ability for the additional training data, another input was used in the training: the freestream velocity. This improves the mapping of I/O relationship by removing the ambiguity. The final design of ANN trained with the combined data from the FLC study under the modified training regime is implemented onto the experimental model for testing. Experiments conducted at all flight conditions within the range of the operating envelope demonstrated the ability of the ANN controller to suppress wing rock at all flight conditions within the operating envelop. Figure 9 shows the results at two flight conditions.

**Table 1 Performance of ANN trained at 23-deg AOA with different freestream velocities**

| Velocities where suppression of wing rock achieved, m/s | | | | |
|---|---|---|---|---|
| 21 AOA | 21.5 AOA | 22 AOA | 22.5 AOA | 23 AOA |
| 18–32 | 16–30 | 16–28 | 18–26 | 16–25 |
| 18–32 | 16–32 | 16–18, 24–32 | 16–18, 26–32 | 26–32 |

## Conclusions

In this Note, we have developed a robust FLC to implement the RASB technique of aerodynamic suppression to control wing rock on single delta wing model. Because of the electro-mechanical lag in the control system, it is not feasible to design an ANN controller using a generalized rule base. The I/O data from FLC experiments provided suitable training data for training the ANN. The effectiveness and robustness of the FLC and ANN controller is demonstrated by wind-tunnel experiments, which reveal successful suppression of wing rock within the tested operating envelop. Results obtained verify the experimental design methodology and also highlight the potential of implementing intelligent controllers like FLC and ANN in aircraft systems.

## References

[1]Ng, T. T., Suarez, C. J., and Malcom, G. N., "Forebody Vortex Control for Wing Rock Suppression," *Journal of Aircraft*, Vol. 31, No. 2, 1994, pp. 298–305.

[2]Johari, H., Olinger, D. J., and Fitzpatrick, K. C., "Delta Wing Vortex Control via Recessed Angled Spanwise Blowing," *Journal of Aircraft*, Vol. 32, No. 4, 1995, pp. 804–810.

[3]Wong, G. S., Rock, S. M., Wood, N. J., and Roberts, L., "Active Control of Wing Rock Using Tangential Leading-Edge Blowing," *Journal of Aircraft*, Vol. 31, No. 3, 1994, pp. 659–665.

[4]Pedreiro, N., Rock, S. M., Celik, Z. Z., and Roberts, L., "Roll–Yaw Control at High Angle of Attack by Forebody Tangential Blowing," *Journal of Aircraft*, Vol. 35, No. 1, 1998, pp. 69–77.

[5]Sreenatha, A. G., and Ong, T. K., "Wing Rock Suppression Using Recessed Angle Spanwise Blowing," *Journal of Aircraft*, Vol. 39, No. 5, 2002, pp. 900–903.

[6]Nayfeh, A. H., Elzebda, J. M., and Mook, D. T., "Development of an Analytical Model of Wing Rock for Slender Delta Wings," *Journal of Aircraft*, Vol. 26, No. 8, 1989, pp. 737–743.

[7]Nayfeh, A. H., Elzebda, J. M., and Mook, D. T., "Analytical Study of Subsonic Wing Rock Phenomenon for Slender Delta Wings," *Journal of Aircraft*, Vol. 26, No. 9, 1989, pp. 805–809.

[8]Sreenatha, A. G., and Lim, Y., "Stability and Robustness Analysis of Fuzzy Logic Controller for Wing Rock Suppression," *AIAA Atmospheric Flight Mechanics Conference*, AIAA Reston, VA, 2000, pp. 701–706.

[9]Joshi, S. V., Sreenatha, A. G., and Chandrasekhar, J., "Suppression of Wing Rock of Slender Delta Wings Using a Single Neuron Controller," *IEEE Transactions on Control Systems Technology*, Vol. 6, No. 5, 1998, pp. 671–677.

[10]Chang, W., Joo, Y. H., Pak, J. B., and Chen, G., "Robust Fuzzy-Model-Based Controller for Uncertain Systems," *1999 IEEE International Fuzzy Systems Conference Proceedings*, IEEE Press, Piscataway, NJ, 1999, pp. 486–491.

[11]Venayagamoorthy, G. K., and Harley, R. G., "A Robust Artificial Neural Network Controller for a Turbogenerator when Line Configuration Changes," *Proceedings of the IEEE Africon'99 Conference*, Vol. 2, IEEE Press, Piscataway, NJ, 1999, pp. 917–922.

# Transpiration Boundary Condition for Computational Fluid Dynamics Solutions in Noninertial Reference Frames

Timothy J. Cowan,* Charles R. O'Neill,† and Andrew S. Arena Jr.‡
*Oklahoma State University, Stillwater, Oklahoma 74078*

## Nomenclature

| | | |
|---|---|---|
| $\boldsymbol{n}$ | = | surface normal vector |
| $\boldsymbol{n}'$ | = | deformed surface normal vector |
| $\boldsymbol{r}$ | = | position vector |
| $\boldsymbol{u}$ | = | fluid velocity vector |
| $\boldsymbol{V}_b$ | = | boundary surface velocity vector |
| $\Delta\boldsymbol{r}$ | = | deformation vector |
| $\Omega$ | = | angular velocity matrix |

## Introduction

THE practicality of time-marched computational fluid dynamics (CFD) solutions for the prediction of aeroelastic and aeroservoelastic characteristics has progressed significantly due to continued advancement in computational capability. Such solutions involve the use of Euler or Navier–Stokes fluid dynamic algorithms coupled with a structural dynamics algorithm through boundary conditions. Unfortunately, the solution computational time increases dramatically if the computational domain must be rediscretized to account for moving structural boundary surfaces. The added computational time and the complexity associated with the meshing process diminish the attractiveness of the approach for full aircraft configurations or other applications where a more rapid 'turnaround' is required, such as flight-test support. Although moving meshes and other methodologies such as grid rediscretization are excellent approaches to problems that are not amenable to small-disturbance assumptions, many problems of practical interest are dominated by mean-flow conditions, under which body motions may be represented by small surface perturbations.

Hence, a method of simulating the boundary deformations for the CFD solver, without actually deforming the computational domain, has proven to be an efficient tool for unsteady aeroelastic predictions. A number of references have demonstrated the viability of this approach, known as the transpiration method, for a wide variety of ploblems.[1–9] The transpiration method was first developed by Lighthill to simulate changes in airfoil thickness.[1] Lighthill modified the normal velocity just outside the boundary layer of an airfoil using the method of equivalent sources to simulate the effects of the boundary layer. This technique has also been used for boundary-layer patching with inviscid-flow techniques. More recently, the technique has been used to simulate surface deformation in full potential solution techniques and in steady and unsteady Euler codes.[2–9]

This Note outlines an extension of the basic transpiration approach and applies the method to problems that are cast in a noninertial frame. This extension of the problem allows a significantly larger set of practical problems to be modeled in this manner because unsteady structural and control deflections may be modeled on geometries undergoing large-amplitude motions. Examples include aeroelasticity, aeroservoelasticity of aircraft undergoing large-amplitude flight dynamics maneuvers, and vibration and aeroelastic modeling of propellers, helicopter rotors, and fans.

## Inertial Transpiration

For an aeroelastic CFD solution, the deformed state of the structure is typically defined by a set of structural mode shapes. The mode shapes define a deformation vector for every surface node in the computational domain. Consider the deformed state given by Fig. 1, where the two nodes of an edge have been displaced from their initial position by a deformation vector $\Delta\boldsymbol{r}$.

In a CFD solution, this statically deformed shape can be simulated, without actually deforming the surface grid, by using the deformed normal vector $\boldsymbol{n}'$ when enforcing flow tangency. The original

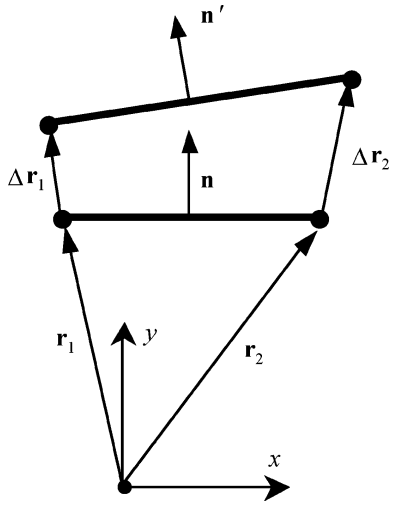


**Fig. 1 Illustration of transpiration concept.**

Received 5 December 2003; accepted for publication 20 January 2004. Copyright © 2004 by the authors. Published by the American Institute of Aeronautics and Astronautics, Inc., with permission. Copies of this paper may be made for personal or internal use, on condition that the copier pay the $10.00 per-copy fee to the Copyright Clearance Center, Inc., 222 Rosewood Drive, Danvers, MA 01923; include the code 0021-8669/04 $10.00 in correspondence with the CCC.

*Aerospace Engineer. Member AIAA.

†Graduate Research Assistant, Mechanical and Aerospace Engineering. Student Member AIAA.

‡L. Andrew Maciula Professor, Mechanical and Aerospace Engineering Department. Senior Member AIAA.